Measurements of correlations enhanced collision rates in the mildly correlated regime ($\Gamma \sim 1$)

F. Anderegg, D. H. E. Dubin, M. Affolter, and C. F. Driscoll
Physics Department 0319, University of California San Diego, La Jolla, California 92093, USA

(Received 7 August 2017; accepted 15 September 2017; published online 28 September 2017)

We measure the perpendicular-to-parallel collision rate $\nu_{\perp||}$ in laser cooled, magnetized ion plasmas in the mildly correlated regime of $\Gamma \sim 1$ and find collision rates enhanced by $\exp(\Gamma)$. This $\nu_{\perp||}$ enhancement due to correlations is directly analogous to the enhancement of fusion collisions in hot dense stellar plasmas, as first analyzed by Salpeter [Aust. J. Phys. **7**, 373 (1954)]. The enhancement is caused by screening of the repulsive Coulomb potential between charges, allowing closer collisions for a given relative energy. The measurements indicate that the screening is done by thermal particles and allows us to rule out dynamical screening theories, which predict no enhancement to the collisions rate for $\Gamma \lesssim 1$. *Published by AIP Publishing*. https://doi.org/10.1063/1.4999350

I. INTRODUCTION

In this paper, we describe the first accurate measurement of the Salpeter correlation enhancement of collision rates in a moderately coupled plasma. The enhancement is caused by plasma screening of the repulsive Coulomb potential between colliding particles, which allows them to have closer collisions for given relative energy. This screening is of importance in astrophysical fusion plasmas.[1]

The present measurements are motivated by competing theories, which predict very different screening factors. The traditional "equilibrium screening" theories[2–7] assume that the plasma response to the colliding particles is static thermal equilibrium Debye screening, and predict a screening enhancement that is an exponentially increasing function of the coupling parameter

$$\Gamma \equiv e^2/a_{ws}T, \tag{1}$$

where e is the ion charge, T is the thermal energy, and $a_{ws} \equiv (3/4\pi n)^{1/3}$ is the mean inter-ion spacing (Wigner-Seitz radius), and n is the density. In contrast, "dynamical screening" theories[8–14] note that colliding pairs move at speeds far above the thermal speed, and postulate altered plasma screening of the pair. Dynamical theories predict almost no screening enhancement for $\Gamma \lesssim 1$, because the plasma cannot respond in time to the fast colliding particles.

Our collision rate measurements strongly contradict dynamical screening theories and show enhancements consistent with the equilibrium screening theories. These measurements are performed in confined near equilibrium pure ion plasmas, for which the coupling parameter Γ is of order one. There are no fusion reactions occurring in such plasma; rather, the measurement relies on an analogy between fusion reaction and energy equipartition. In a strongly magnetized non-neutral plasma for which $\Omega_c \gg \bar{v}/b$, where $\Omega_c \equiv eB/mc$ is the cyclotron frequency, $\bar{v} \equiv (T/m)^{1/2}$ is the thermal speed, $b = e^2/T$ is the distance of closest approach, and the kinetic energy associated with the perpendicular cyclotron motion is an adiabatic invariant. This cyclotron energy is shared with other degrees of freedom only through close collision of supra-thermal particles that break the adiabatic invariant. Similarly, nuclear energy is shared with other degrees of freedom only through close, energetic collisions. The enhancement of perpendicular-to-parallel collisions has been shown to be identical to the enhancement of nuclear reactions, because both enhancements involve the same plasma screening of close collisions of supra-thermal particles.[15]

In previous work, the enhancement factor was measured and found to be consistent with equilibrium screening theories in the region $\Gamma < 15$, with enhancement up to 10^9.[16,17] This new work provides higher accuracy measurements for $\Gamma \lesssim 1$ in order to compare to dynamical theories which predict negligible enhancement when Γ is small.

In a broader context, this enhancement of $\nu_{\perp||}$ is but one of several interesting plasma correlation effects. Experiments and theory on un-neutralized ion plasmas have analyzed the equilibrium crystal structures occurring for $\Gamma \gtrsim 200$, including the near-equilibrium oscillatory modes and unusual "stick/slip" effects.[18] Unexpected "explosive re-heating" of laser cooled crystal due to equilibration of cyclotron motion with motion parallel to the magnetic field is more than 10 orders of magnitude faster than that predicted by theory neglecting correlations.[19] The broad range of non-equilibrium transport effect such as particle and heat diffusion and viscosity remain relatively un-explored experimentally in the correlated regime, but amenable to molecular dynamics simulations.[20] Recent experiments on ultra-cold quasi-neutral plasmas have measured test-particle velocity relaxation rates during self-similar expansion with ion-ion correlation parameter $\Gamma \sim 1$.[21] In "dusty plasma" experiments, planar crystal equilibria and waves are accurately measured on visible particles, charged and shielded by the background plasma.[22]

II. EFFECT OF CORRELATIONS ON COLLISION RATE

In a strongly magnetized plasma with a perpendicular temperature $T_\perp$ and a parallel temperature $T_{||}$, the perpendicular-to-parallel collision rate $\nu_{\perp||}$ is defined as

$$\frac{d}{dt}T_\perp = \nu_{\perp||}(T_{||} - T_\perp), \tag{2}$$

with

$$\nu_{\perp||} \equiv n\bar{v}b^2\, 4\sqrt{2} I(\bar{\kappa})\, g(\Gamma). \tag{3}$$

Here, the "bare" collision rate $4\sqrt{2}\, n\bar{v}b^2$ is modified by a dynamical factor $I(\bar{\kappa})$ depending only on the magnetization parameter

$$\bar{\kappa} \equiv \sqrt{2}\, \frac{b}{r_c}, \tag{4}$$

and also modified by a correlation factor $g(\Gamma)$, which depends only on the correlation parameter Γ. Here $r_c \equiv \bar{v}/\Omega_c$ is the cyclotron radius and $\bar{v} \equiv \sqrt{T/m}$ is the particle thermal speed.

This dynamical factor $I(\bar{\kappa})$ suppresses the perpendicular-to-parallel collision rate in the strongly magnetized regime of $\bar{\kappa} > 1$. In this regime, only rare energetic collisions mix the perpendicular energy $E_\perp$ and parallel energy $E_{||}$. The correlation factor $g(\Gamma)$ enhances these rare collisions due to particle correlations in the cryogenic liquid regime of $0.1 \lesssim \Gamma \lesssim 10$.

A. Strong magnetization

Here, we briefly review the strong magnetization regime results. A rigorous derivation can be found in Ref. 23. For $\bar{\kappa} > 1$, the perpendicular energy of two particles is an adiabatic invariant. That is, $E_\perp = E_{\perp 1} + E_{\perp 2}$ is conserved by most collisions, except for rare energetic (large $E_{||}$) collisions. The cross-section σ for sharing perpendicular and parallel energy is a function of $E_{||}$

$$\sigma(E_{||}) \propto \exp\left[-\pi\left(\frac{b}{r_c}\right)\right] \approx \exp\left[-\pi\left(\frac{C}{E_{||}}\right)^{\frac{3}{2}}\right], \tag{5}$$

where C is a constant. That is, the cross-section for $E_{||} - E_\perp$ sharing increases exponentially for large $E_{||}$. The collision rate is obtained by integrating the product of the Maxwellian particle distribution and $\sigma(E_{||})$.

$$\nu_{\perp||}^{\text{no corr}} = \int dE_{||}\, \frac{1}{T}\, \exp\left(-\frac{E_{||}}{T}\right)\sigma(E_{||}) = n\bar{v}b^2 4\sqrt{2} I(\bar{\kappa}), \tag{6}$$

where $I(\bar{\kappa})$ can be approximated as[23]

$$I(\bar{\kappa}) \approx 1.5\, \exp\left(-2.044\, \bar{\kappa}^{\frac{2}{5}}\right). \tag{7}$$

Thus, most of the collisions causing sharing of $E_{||}$ and $E_\perp$ come from the "Gamow" peak, as shown in Fig. 1. For example, the Gamow peak is located at 4 $\bar{v}$ for $\bar{\kappa} = 20$, so less than 2% of the particles participate in such "rare" collision. The cyclotron energy is released only by rare collisions, analogous to fusion reactions where the energy stored in the nuclei is liberated only by rare energetic collisions.

B. Correlations

Correlations enhance the perpendicular-to-parallel collision rate, through screening effects, which reduce the amount of parallel energy required for two ions to come within a distance ρ. In the absence of shielding, the energy required is

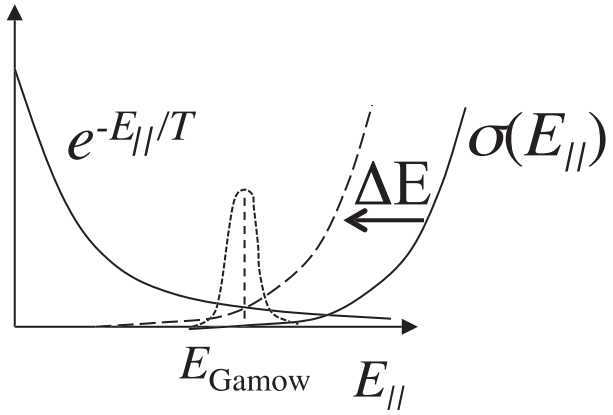

FIG. 1. Graphic description of the integrand of Eq. (6) showing exponentially decaying Maxwellian particle energy distribution and the exponentially growing cross-section σ. The product of the particle distribution and the cross-section gives rise to the Gamow peak. Shifting σ by ΔE gives enhancement $\exp(\Delta E/T)$.

$$E_{||} = \frac{e^2}{\rho}\,. \tag{8}$$

In contrast, with Debye screening the parallel energy required is smaller, as

$$E_{||} = \frac{e^2}{\rho}\, \exp\left(\frac{-\rho}{\lambda_D}\right) \simeq \frac{e^2}{\rho} - \frac{e^2}{\lambda_D}\,. \tag{9}$$

In the strong coupling regime of $\Gamma > 1$, the effective shielding distance λ is the inter-particle spacing a_{ws}, and the energy required for a collision at distance $\rho < a_{ws}$ is

$$E_{||} \simeq \frac{e^2}{\rho} - \frac{e^2}{a_{ws}}\,. \tag{10}$$

This shifts the cross-section $\sigma(E_{||})$ by $\Delta E_{||} = e^2/a_{ws}$, as shown in Fig. 1. Equivalently, the Maxwellian in Eq. (6) is shifted by $\Delta E_{||}/T = e^2/(a_{ws}T) = \Gamma$. Therefore, Eq. (6) becomes

$$\begin{aligned}\nu_{\perp||}^{corr} &\simeq \int dE_{||}\, \frac{1}{T}\, \exp\left(-\frac{E_{||}}{T} - \frac{e^2}{a_{ws}T}\right)\sigma(E_{||}) \\ &= \exp\left(\frac{e^2}{a_{ws}T}\right)\int dE_{||}\, \frac{1}{T}\, \exp\left(-\frac{E_{||}}{T}\right)\sigma(E_{||}) \\ &= \exp(\Gamma)\, \nu_{\perp||}^{no\ corr}\,.\end{aligned} \tag{11}$$

Correlations increase the perpendicular-to-parallel collision rate by a factor of roughly $g(\Gamma) = \exp(\Gamma)$. It is worth noting that the enhancement is independent of $\sigma(E)$, as in the fusion case, where this effect is known as the Salpeter enhancement.

A rigorous derivation of $g(\Gamma)$ for non-neutral plasmas can be found in Ref. 15, and a comprehensive review of the correlation enhancement for stellar nuclear fusion is presented in Table II of Chugunov.[2]

Note that theory assumes that $f(v)$ is a two-temperature Maxwellian, but equipartition occurs dominantly for high energy particles, which can drive the system away from Maxwellian.

However, in the gamma range of the experiments in this paper (i.e., $\Gamma \gtrsim 0.1$), we believe that three-body collisions can keep the parallel distribution close to Maxwellian at rate that is faster than the exponentially small equipartition rate that drives the high energy particles away from a Maxwellian. (In previous electron experiments[24] with $\Gamma \ll 1$, this is not true and high energy particles may indeed be driven away from Maxwellian. The importance of this effect remains an open question.)

III. EXPERIMENTS

These experiments are conducted using a magnesium ion plasma confined in a Penning-Malmberg trap with a magnetic field of $B = 1.2$ T and a wall radius $R_W = 2.86$ cm.[25] The cylindrical plasma column has density $n \simeq 2 \times 10^7$ cm^{-3}, length $L_p = 11$ cm, and a radius $R_p \simeq 0.3$ cm. A weak "rotating wall" electric field confines the plasma in steady state for weeks.[26] The plasma density n and temperatures $T_{||}$ and $T_\perp$ are diagnosed with Laser Induced Fluorescence. The laser frequency is scanned across the $S_{1/2}$, $m_j = +1/2 \rightarrow P_{3/2}$, $m_j = +3/2$ transition ($\lambda \simeq 280$ nm) and the fluorescence is recorded. This transition measures the population of the ground state of the magnesium ions. The fluorescence signal versus laser frequency is fit to a "Voigt" profile encompassing the Lorentzian natural line-width of the optical transition and the Maxwellian distribution due to Doppler broadening from thermal motion. The temperature is controlled by a parallel laser beam resulting in temperature $10^{-5} < T < 10^{-3}$ eV for the data presented here. We obtain $\Gamma = 1$ for density $n \simeq 2 \times 10^7$ cm^{-3} and temperature $T \simeq 6 \times 10^{-5}$ eV.

To measure the collision rate $\nu_{\perp||}$, we use the "optimal frequency" technique,[16,17,24] determining the compression/expansion frequency at which axial compressions give maximal heating. The plasma is axially compressed and expanded by a burst of a few cycles (typically 3 to 100) at frequency f_{osc} applied to an electrode located near one end of the plasma column. Typically, $\delta L_p/L_p \approx 10^{-4}$ in each cycle. The frequency f_{osc} resulting in maximal heating occurs when

$$\nu_{\perp||} = 2\pi f_{osc}\, c(\Gamma), \tag{12}$$

here $c(\Gamma) = c_{||}c_\perp/(c_{||} + c_\perp)$ is the plasma specific heat at constant density, with $c_\perp = 1$ and $c_{||} = 1/2 + \frac{\partial U_{corr}}{\partial T}$, and the correlation energy U_{corr} is defined in equation 4.24 of Ref. 27 and varies mildly with correlation, with $c(0) = 1/3$, $c(2) \simeq 0.42$ and $c(10) \simeq 0.52$. To detect the plasma heating, we monitor the fluorescence of the large diameter cooling beam as f_{osc} is changed. The largest change in fluorescence determines the collision rate.

Figure 2 shows the measured collision rate $\nu_{\perp||}$ for $10^{-5} < T < 10^{-3}$ eV. The collision rate decreases by a factor of 10 when the plasma is strongly magnetized ($\bar{\kappa} > 1$). The solid line is the theory prediction of $\nu_{\perp||}^{no\,corr}$ from Eq. (6), using numerical values for $I(\bar{\kappa})$ from Ref. 23 with no adjustable parameters. The dashed line is the theory prediction for $\nu_{\perp||}^{corr}$ as calculated by Gasques[3] from Montecarlo simulation of DeWitt and Slatery[7] giving

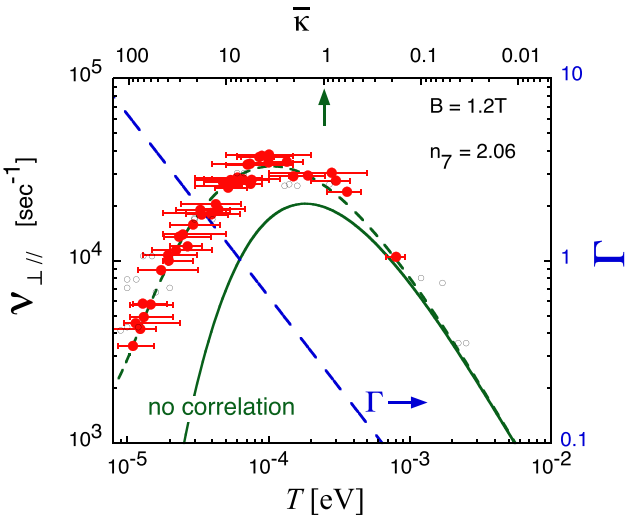

FIG. 2. Measured perpendicular to parallel collision rate $\nu_{\perp||}$ versus temperature T compared to Eq. (13) with no adjustable parameters. The top horizontal axis shows the magnetization parameter $\bar{\kappa}(T)$, and the correlation parameter $\Gamma(T)$ is plotted with a long dashed line.

$$\ln(g(\Gamma)) = 1.0563\Gamma + 1.0208\Gamma^{0.3231} - 0.2748\ln\Gamma - 1.0843. \tag{13}$$

The plotted temperature T is the density-weighted average of the measured temperature profile. A $T(r)$ profile is obtained for each $\nu_{\perp||}$ measurement and typically consists of measurements at 21 radial locations. The temperature "error bars" represent the lowest and highest temperatures in the radial profile. The error on the measured optimal frequency is negligible and is typically smaller than the size of the symbol on the plot.

The data demonstrate that correlations are increasing the collision rate when the system starts developing correlations. For reference, older data[17] are shown with open symbols. The temperature scatter of the new data has been reduced at low temperatures through improved long term laser frequency stability.

Figure 3 re-plots the data of Fig. 2 to show the enhancement of the collision rate due to correlations, as $g(\Gamma) \equiv \nu_{\perp||}/\nu_{\perp||}^{no\,corr}$ showing the basic $\exp(\Gamma)$ dependence of Eq. (11). Here, the temperature "error bars" for each measured $\nu_{\perp||}$ are represented by separate symbols, and the highest temperature in the profile (smaller gamma) is plotted with open diamonds, while the lowest measured temperature is plotted with the open triangles. We have previously verified that the enhancement $g(\Gamma)$ is independent of the magnetic field,[17] while the dynamical factor $I(\bar{\kappa})$ depends on the magnetic field.

Figure 4 shows $g(\Gamma)$ plotted on an expanded linear scale to show more clearly the various theory predictions. The dashed line on Figs. 3 and 4 is Eq. (13). The dot-dashed line is the original analytic expression of DeWitt and Slattery[7] for $\Gamma > 1$

$$\ln(g(\Gamma)) = 1.056299\Gamma + 1.039957\Gamma^{0.323064} - 0.5455823\ln\Gamma - 1.1323. \tag{14}$$

The solid line is an analytical approximation computed by Jancovici[4] for $\Gamma > 1$, and is almost undistinguishable from Eq. (13) over the range of Γ plotted.

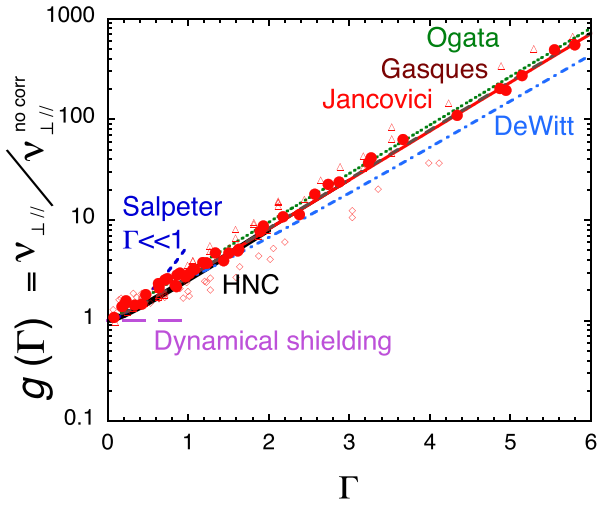

FIG. 3. Collision rate enhancement plotted versus the correlation parameter.

$$\ln(g(\Gamma)) = 1.0531\Gamma + 2.2931\Gamma^{1/4} - 0.5551\ln\Gamma - 2.35. \tag{15}$$

The dotted line is an analytical approximation computed by Ogata[5] for $\Gamma > 1$

$$\ln(g(\Gamma)) = 1.132\Gamma - 0.0094\Gamma\ln\Gamma. \tag{16}$$

All these equilibrium screenings with no adjustable parameter estimates are consistent with the present measurements over the range of Γ presented here. The theories of Gasques Eq. (13) and Jancovici Eq. (15) are in closest quantitative agreement with the data. For completeness, we have also plotted the original Salpeter prediction valid for the weak screening $\Gamma \ll 1$.

$$\ln(g(\Gamma)) = \sqrt{3}\,\Gamma^{3/2}, \tag{17}$$

and in the strong screening regime, the original Salpeter prediction (not shown on Figs. 3 and 4) is

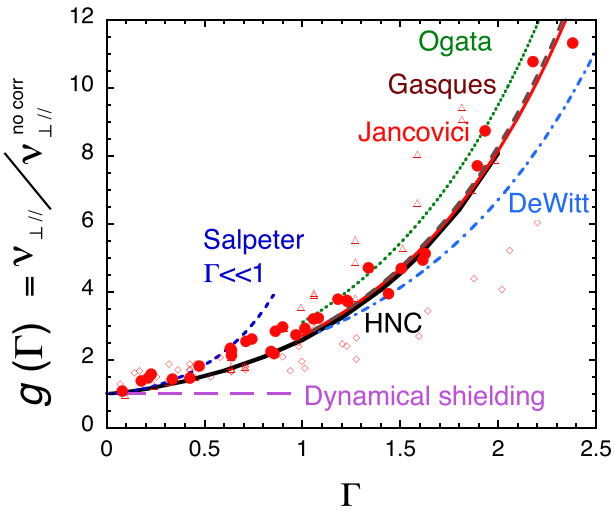

FIG. 4. Collision rate enhancement plotted versus the correlation parameter on expanded scale.

$$\ln(g(\Gamma)) = 0.9(2^{5/3} - 2)\Gamma = 1.0573\,\Gamma. \tag{18}$$

The solid black curve (HNC) running from $\Gamma = 0$ to $\Gamma = 2$ in Figs. 3 and 4 represents "statistical potential" theory appropriate to $\Gamma \sim 1$. In equilibrium screening theory, the screening enhancement factor $g(\Gamma)$ is related to the classical radial distribution function $G(\rho)$ by writing $G(\rho)$ as[6]

$$G(\rho) = \exp\left(-(e^2/\rho - H(\rho))/T\right), \tag{19}$$

where $H(\rho)$ is a statistical 2-body potential. The enhancement factor is then given by

$$g(\Gamma) = \exp\left(H(0)/T\right). \tag{20}$$

That is, $g(\Gamma)$ is the enhancement of the contact probability for two repulsive charges in a one component plasma over and above the vacuum correlation factor $\exp\left(-e^2/(\rho T)\right)$. For small-to-moderate values of Γ, the function $H(\rho)$ can be directly evaluated using the well-known Hyper Netted Chain (HNC) equations,[28] which have been shown previously[29,30] to provide good approximations for the correlation function for moderate Γ value. By applying the iterative approach to the solution of these equations described in Ref. 31, we have evaluated $g(\Gamma) = \exp\left(H(0)/T\right)$ for a range of Γ values from $0 < \Gamma < 2$; and this is plotted with a thick solid black line on Figs. 3 and 4.

In contrast, dynamical shielding theories[8–14] predict no enhancement for $0 < \Gamma < 1$, as shown by the long dashed line on Figs. 3 and 4. The present data preclude such theories. Prior theoretical arguments against dynamical shielding theory have been previously presented by Bahcall.[32]

ACKNOWLEDGMENTS

The authors acknowledge many fruitful discussions with Tom O'Neil. This work has been supported by National Science Foundation Grant No. PHY-1414570 and Department of Energy Grant Nos. DE-SC0002451 and DE-SC0008693.

[1]E. E. Salpeter, Aust. J. Phys. **7**, 373 (1954).
[2]A. I. Chugunov, H. E. DeWitt, and D. G. Yakolev, Phys. Rev. D **76**, 025028 (2007).
[3]L. R. Gasques, A. V. Afanasjev, E. F. Aguilera, M. Beard, L. C. Chamon, P. Ring, M. Wiescher, and D. G. Yakovlev, Phys. Rev. C **72**, 025806 (2005).
[4]B. Jancovici, J. Stat. Phys. **17**, 357 (1977).
[5]S. Ogata, Astrophys. J. **481**, 883 (1997).
[6]S. Ichimaru, Rev. Mod. Phys. **65**, 255 (1993).
[7]H. Dewitt and W. Slattery, Contrib. Plasma Phys. **39**, 97 (1999).
[8]N. J. Shaviv and G. Shaviv, Astrophys. J. **468**, 433 (1996).
[9]C. Carraro, A. Schafer, and S. E. Koonin, Astrophys. J. **331**, 565 (1988).
[10]A. Lavagno and P. Quarati, Nucl. Phys. B (Proc. Suppl.) **87**, 209 (2000).
[11]G. Shaviv and N. J. Shaviv, Astrophys. J. **529**, 1054 (2000).
[12]V. N. Tsytovich, Astron. Astrophys. **356**, L57 (2000).
[13]V. I. Savchenko, Phys. Plasmas **8**, 82 (2001).
[14]W. Dappen and K. Mussack, Contrib. Plasma Phys. **52**, 149 (2012).
[15]D. H. E. Dubin, Phys. Plasmas **15**, 055705 (2008); Phys. Rev. Lett. **94**, 025002 (2005).
[16]F. Anderegg, D. H. E. Dubin, T. M. O'Neil, and C. F. Driscoll, Phys. Rev. Lett. **102**, 185001 (2009).
[17]F. Anderegg, C. F. Driscoll, D. H. E. Dubin, and T. M. O'Neil, Phys. Plasmas **17**, 055702 (2010).

[18]T. B. Mitchell, J. J. Bollinger, W. M. Itano, and D. H. E. Dubin, Phys. Rev. Lett. **87**, 183001 (2001).
[19]M. J. Jensen, T. Hasegawa, J. J. Bollinger, and D. H. E. Dubin, Phys. Rev. Lett. **94**, 025001 (2005).
[20]S. D. Baalrud and J. Daligaut, Contrib. Plasma Phys. **57**, 238–251 (2017).
[21]T. S. Strickler, T. K. Langin, P. McQuillen, J. Daligault, and T. C. Killian, Phys. Rev. X **6**, 021021 (2016).
[22]H. Thomas, G. E. Morfill, V. Demmel, J. Goree, B. Feuerbacher, and D. Mohlmann, Phys. Rev. Lett. **73**, 652 (1994).
[23]M. E. Glinsky, T. M. O'Neil, M. N. Rosenbluth, K. Tsuruta, and S. Ichimaru, Phys. Fluids B **4**, 1156 (1992).
[24]B. R. Beck, J. Fajans, and J. H. Malmberg, Phys. Plasmas **3**, 1250 (1996). Phys. Rev. Lett. **68**, 317 (1992).
[25]F. Anderegg, X.-P. Huang, E. Sarid, and C. F. Driscoll, Rev. Sci. Instrum. **68**, 2367 (1997).
[26]X.-P. Huang, F. Anderegg, E. M. Hollmann, C. F. Driscoll, and T. M. O'Neil, Phys. Rev. Lett. **78**, 875 (1997). E. M. Hollmann, F. Anderegg, and C. F. Driscoll, Phys. Plasmas **7**, 2776 (2000).
[27]D. H. E. Dubin and T. M. O'Neil, Rev. Mod. Phys. **71**, 87 (1999).
[28]F. Lado, J. Comput. Phys. **8**, 417 (1971).
[29]S. Cooper, Phys. Rev. A **7**, 1 (1973).
[30]J. F. Springer, M. A. Pokrant, and F. A. Stevens, Jr., J. Chem. Phys. **58**, 4863 (1973).
[31]K.-C. Ng, J. Chem. Phys. **61**, 2689 (1974).
[32]J. N. Bahcall, L. S. Brown, A. Gruzinov, and R. F. Sawyer, Astron. Astrophys. **383**, 291 (2002).